International Journal of Rock Mechanics & Mining Sciences 48 (2011) 187–198

Contents lists available at ScienceDirect

International Journal of Rock Mechanics & Mining Sciences

journal homepage: www.elsevier.com/locate/ijrmms

Semi-automatic extraction of rock mass structural data from high resolution LIDAR point clouds

Giovanni Gigli [a,*], Nicola Casagli [b,1]

[a] Department of Earth Sciences, University of Florence, Largo Enrico Fermi 2, Arcetri, 50125, Florence, Italy
[b] Department of Earth Sciences, University of Florence, Via Giorgio La Pira 4, 50121, Florence, Italy

ARTICLE INFO

Article history:
Received 8 October 2009
Received in revised form
26 June 2010
Accepted 27 November 2010
Available online 5 January 2011

Keywords:
Geomechanical survey
Automatic
Matlab
Laser scanning
Point cloud
DiAna

ABSTRACT

In this paper a Matlab tool called DiAna (Discontinuity Analysis), for the 2D and 3D geo-structural analysis of rock mass discontinuities on high resolution laser scanning data is presented.

The proposed approach is able to semi-automatically retrieve some relevant rock mass parameters, namely orientation, number of sets, spacing/frequency (and derived RQD), persistence, block size and scale dependent roughness, by analyzing high resolution point clouds acquired from terrestrial or aerial laser scanners.

In addition, with a specific DiAna option called *filterveg*, we are able to remove vegetation or other disturbing objects from the point cloud, which is one of the main problems in LIDAR data processing.

Some examples of the proposed method have demonstrated its ability to investigate rock masses characterized by irregular block shapes, and suggest applications in the field of engineering geology and emergency management, when it is often advisable to minimize survey time in dangerous environments and, in the same time, it is necessary to gather all the required information as fast as possible.

1. Introduction

When we face engineering geology problems in rock, it is fundamental to reconstruct the 3D geometry and the structural setting of the rock masses, sometimes in inaccessible areas. An accurate description of the geometrical and mechanical properties of the material is specifically required, as the overall mechanical behavior of a rock mass depends on its structure, on the characteristics of discontinuities and on the properties of intact rock.

Traditional geomechanical surveys are performed in situ, either in one dimension (scanline method) or two dimensions (window method), and require direct access to the rock face for the collection of the relevant parameters [1].

ISRM [2] selected the following ten parameters for the quantitative description of discontinuities in rock masses: orientation, spacing, persistence, roughness, wall strength, aperture, filling, seepage, number of sets, and block size.

For practical and safety reasons, traditional geomechanical surveys are often carried out on limited sectors of the rock mass, and usually they do not provide data for a complete reconstruction of the full variability of a rock mass.

Nowadays, several techniques are available for retrieving high resolution 3D representations of land surface, such as digital photogrammetry [3,4], laser scanning (terrestrial and aerial) [5,6] and SAR interferometry [7].

In addition, the increased computational performance of personal computers allows us to process large amounts of data in a relatively short time.

The advantage of employing remote and high resolution surveying techniques for geomechanical purposes is based on the capability of performing both large scale [8,9] and small scale [10,11] analyses and to rapidly obtain information on inaccessible rock exposures.

Sometimes, the features of interest can be very large [12], and they could actually remain unnoticed if only a small scale field survey is performed. On the other side, the observation of small details, such as discontinuity planes or traces and surface roughness, is a key element for the geomechanical characterization of the rock mass.

In order to perform correct analyses from a statistical point of view, we need, therefore, to investigate a portion of the rock face as wide as possible.

The capability of capturing small details depends primarily on the resolution and on the accuracy of the survey method.

The main product of a long range laser scanning survey [13] is a high resolution point cloud, obtained by measuring with high accuracy (millimetric or centimetric) the distance of a mesh of points on the object, following a regular pattern with polar coordinates. The high

* Corresponding author. Fax: +39 055 2055317.
E-mail addresses: giovanni.gigli@unifi.it (G. Gigli), nicola.casagli@unifi.it (N. Casagli).
[1] Fax: +39 055 2756296.

1365-1609/$ - see front matter © 2010 Elsevier Ltd. All rights reserved.
doi:10.1016/j.ijrmms.2010.11.009

acquisition rate (up to hundreds of thousands of points/s) allows to immediately obtain the detailed 3D shape of the object.

Laser scanning data can be processed by true coloring point clouds from high resolution optical digital images, or by triangulating points in order to create Digital Surface Models (DSM).

One of the main tasks when we have to interpret the acquired data is the vegetation removal [14].

Two main different levels of automation can be conceived, to extract the most relevant rock mass geomechanical characteristics, hidden in the point cloud.

- *Manual*: by inspecting the point cloud or the derived surface, fitting local planes, taking measurements, drawing polylines of interest, etc. [15]. This procedure has, however, a non-systematic character, is time-consuming and tends to neglect the smallest features. It is a subjective or biased analysis, as only those discontinuities, which appear to be important are investigated. The success of this approach depends on the quality of digital data and on the skill and experience of the geologist.
- *Automatic/semi-automatic*: by selecting a specific algorithm for the segmentation of the original data in clusters of points belonging to the same discontinuity. This can be defined as an objective or random analysis, since all detectable discontinuities within the surveyed area are sampled. Since raw data can contain up to tens of millions of points, the adopted algorithm should be optimized to make computational time acceptable. In the author's opinion, it is important to use both approaches, because they can complement each other.

In this paper we present a Matlab tool called DiAna (Discontinuity Analysis), for the 2D and 3D semi-automatic extraction of rock mass structural information from high resolution point clouds obtained from a terrestrial laser scanner.

In particular, six of the ten ISRM [2] parameters can be evaluated (orientation, number of sets, spacing/frequency, persistence, block size and scale dependent roughness) and a specific option for vegetation removal (*filterveg*) is implemented.

After a review of the state of the art for indirect rock face characterization, both 2D and 3D versions of the proposed tool are described, and a field application is presented to validate the semi-automatically obtained results with traditional field survey data.

2. Methods for indirect rock face characterization

During the last years many authors have been working on the extraction of 3D rock mass properties from remotely acquired high resolution data, mainly digital photogrammetry and LIDAR [16–25].

These efforts led to the development of specific tools or software, written either for personal research or commercial purposes: i.e. Vulcan [26]; Jointmetrix3D [27]; Surpac [28]; Sirovision [29]; 3DM Analyst [30]; Split-FX [31]; 3DGeomec [32]; Coltop3D [20].

Since laser scanning is a more recent technique than digital photogrammetry, the software currently available for the latter application is more advanced [33] and there are many commercial packages that include geological and structural mapping facilities [34–36].

With the aim of semi-automatically extracting the geometrical characteristics of a rock mass from Lidar data, two basic approaches can be pursued, by working on point clouds or derived surfaces.

First of all, since our primary object is the estimation of discontinuity plane orientations and the comparison with field measurements, the raw data have to be georeferenced on a global reference system, in order to obtain true orientations of the surfaces of interest with respect to the horizontal (dip) and North (dip direction).

The creation of a surface from a point cloud leads to a simplification and a first segmentation of the original data in elementary polygons (usually triangles), whose spatial location and orientation can be calculated. It is therefore possible to group neighbor polygons with similar orientation, and to individuate the extent of planar features within the investigated object [17,18,23].

However, the capability of reconstructing discontinuity surfaces depends primarily on the quality of the triangulation process and its resolution. Small features can be neglected, and complex shapes could lead to incorrect and distorted polygonal surfaces.

On the other side, working on raw point cloud data gives the advantage of keeping all the initial information, and the disadvantage of a larger amount of input data to be processed, with a consequently longer computational time.

This approach has been adopted by Jaboyedoff et al. [20] for the assessment of the local orientation of ground surface, and for vegetation detection and removal, by means of eigenvalues.

Roncella et al. [16], Voyat et al. [19] and Ferrero et al. [22] applied a procedure based on the Random Sample Consensus (RANSAC) algorithm [37] for the segmentation of point clouds into subsets, each made of points belonging to the same discontinuity surface.

Slob et al. [21] proposed a method for the direct segmentation of point clouds, by verifying if most of the points around a seed point lie close to the same flat plane. Should this happen, the operation is iterated by selecting other neighboring points and verifying their position with respect to the plane found before, in order to individuate the extent of the discontinuity surface.

3. Proposed method

In this paper, for the 3D semi-automatic analysis of large point clouds finalized to the extraction of the geomechanical characteristics of rock masses, we propose a new approach based on the definition of least squares fitting planes on clusters of points extracted by moving a sampling cube on the point cloud. By selecting the cube dimension and a standard deviation threshold, the adopted method has demonstrated its validity to investigate even rock masses characterized by very irregular block shapes.

The advantage of using this approach lies in its capability to investigate all the geomechanical parameters that do not require direct access to the rock mass, thus, making this a more complete analysis in connection with the existing methods described in the previous section. The output ISRM [2] parameters are: orientation, number of sets, spacing/frequency (and derived RQD), persistence, block size and scale dependent roughness.

With the aim of keeping all the original information, the input data of the proposed algorithm are unorganized point clouds, produced by merging data acquired from different positions or even diverse techniques, in order to avoid shadow areas and to obtain a regular distribution of points. The heterogeneity of point clouds consequently is one of the main limitations of the employment of ground-based laser scanning in rock slope characterization, as outlined by Sturzenegger et al. [38].

Natural and man-made slopes show, however, very different morphology, which results in different processing conceptions.

Often, especially in case of man-made excavations, the rock slope face is planar. In these circumstances, only discontinuity traces are detectable from the point cloud, provided the available data are associated with a digital image and their resolution is high enough. Discontinuity traces can be represented by 2D polylines on the slope fitting plane, and a 2D quantitative analysis can be performed, based on their length and their pitch angle on the reference plane, the orientation of which is known.

On the other side, rock faces with rugged shape can be investigated by inspecting the discontinuity surfaces exposed on the slope. Such 3D approach requires the extraction of clusters of points belonging to the same discontinuity plane from the point cloud; subsequently, a spatial analysis for the quantitative description of discontinuities within the rock mass has to be performed.

Both cases have been dealt with the proposed method, by applying two different Matlab [39] tools, called DiAna3D and DiAna2D and fully described in the following sections.

Authors are presently working at the integration of the 2D and 3D methods in a single tool, after which their intent is to distribute it for free.

3.1. DiAna3D

The three dimensional approach is based on the selection of a sub-set of the point cloud (red points in Fig. 1) contained within a searching cube (red cube in Fig. 1).

The best fitting plane (blue grid in Fig. 1) according to the least squares method is then found for the cubic selection, by applying the singular value decomposition matlab function (svd) [40].

The plane is defined by its direction cosines (l, m, n) and has a general equation of the type

$$ax+by+cz+d=0 \tag{1}$$

The standard deviation (σ) of the selected points concerning the best fitting plane is then computed and a threshold value (σ_t) is chosen by the user, based on the searching cube dimension, the resolution of the point cloud and the large scale roughness characteristics of the rock slope.

If $\sigma<\sigma_t$ a *cluster* is formed and the selected points are extracted from the point cloud. A minimum number of points within the selection cube can be chosen, to avoid the formation of small and unrepresentative clusters.

In order to cover the whole point cloud, the searching cube is moved along the geographic axes according to a regular pattern (*box* analysis; Fig. 2), or can be centered at each single point of the point cloud (*discrete* analysis).

Once a valid cluster has been identified, the associated plane orientation is found by applying the following equations [1]:

$$\alpha=\arctan\left(\frac{m}{l}\right)+Q \tag{2}$$

$$\beta=\arctan\left(\frac{n}{\sqrt{l^2+m^2}}\right) \tag{3}$$

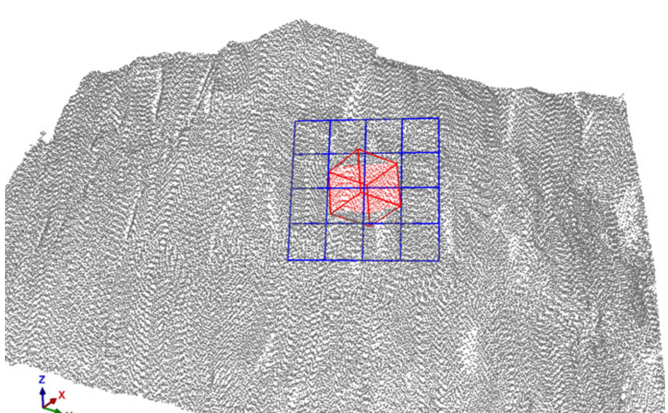

Fig. 1. Cubic selection (red points) and best fitting plane (blue grid) on high resolution point cloud. The dimension of the red selection cube is 1 m. (For interpretation of the references to color in this figure legend, the reader is referred to the web version of this article.)

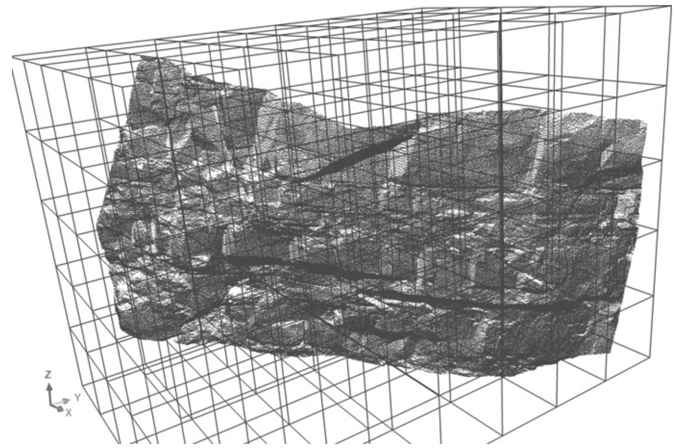

Fig. 2. Example of box analysis with a 2 m reference cube. A sub-set of the point cloud contained within each cube is recursively selected for the definition of the best fitting plane.

where α and β are the plane dip/direction and dip, respectively; l, m and n are the direction cosines of the plane; Q is a constant, which assumes the following values: $Q=0^\circ$ if $l>0$ and $m>0$; $Q=360^\circ$ if $l>0$ and $m<0$; $Q=180^\circ$ if $l<0$ and $m<0$ or if $l<0$ and $m>0$.

The adopted procedure allows both to isolate those points belonging to a planar surface and to make local face orientation measures, just like moving with a compass and clinometer on the rock face, taking measurements on discontinuity planes.

Different searching cube dimensions can be selected; the smaller is the cube dimension, the smaller is the feature that can be observed on the point cloud (Fig. 3).

All cluster orientations are then plotted on the stereographic projection. Fig. 4 shows the stereoplot of the clusters extracted with a reference cube dimension of 0.1 m (Fig. 3d), with a total of 18,757 poles.

The main discontinuity sets can therefore be extracted from the point cloud (Fig. 5), as all the clusters belonging to the same set are assigned a common ID. In order to directly control the set recognition process, and to have an immediate validation with possible field data, we chose to perform this operation manually; for this reason the whole 3D approach can be defined as semi-automatic.

The next step is aimed at merging all the clusters belonging to the same discontinuity plane. This is done by comparing the orientation of all neighboring clusters with the set they belong to: if two clusters with similar orientation (same set) have been extracted from adjoining cubes, they are supposed to belong to the same discontinuity surface.

Based on this assumption a small enough reference cube dimension has to be chosen to avoid the method to group together two closely spaced parallel discontinuities.

This operation can be iterated by considering all the clusters the centroids of which fall within a fixed distance each other, to obtain the maximum extent of single discontinuity faces.

In order to fill holes, isolated clusters with unassigned ID are attributed to a discontinuity plane if they are surrounded by clusters assigned to the same discontinuity surface.

Fig. 6 reports the results of the merging process for the clusters extracted with a 0.1 m reference dimension. A total of 79 discontinuity surfaces have been identified by merging 18,757 clusters (Figs. 3d and 4).

By applying this procedure it is possible to extract even minor discontinuity planes. Fig. 6 demonstrates that decimetric features can be observed, if the searching cube dimension is small enough.

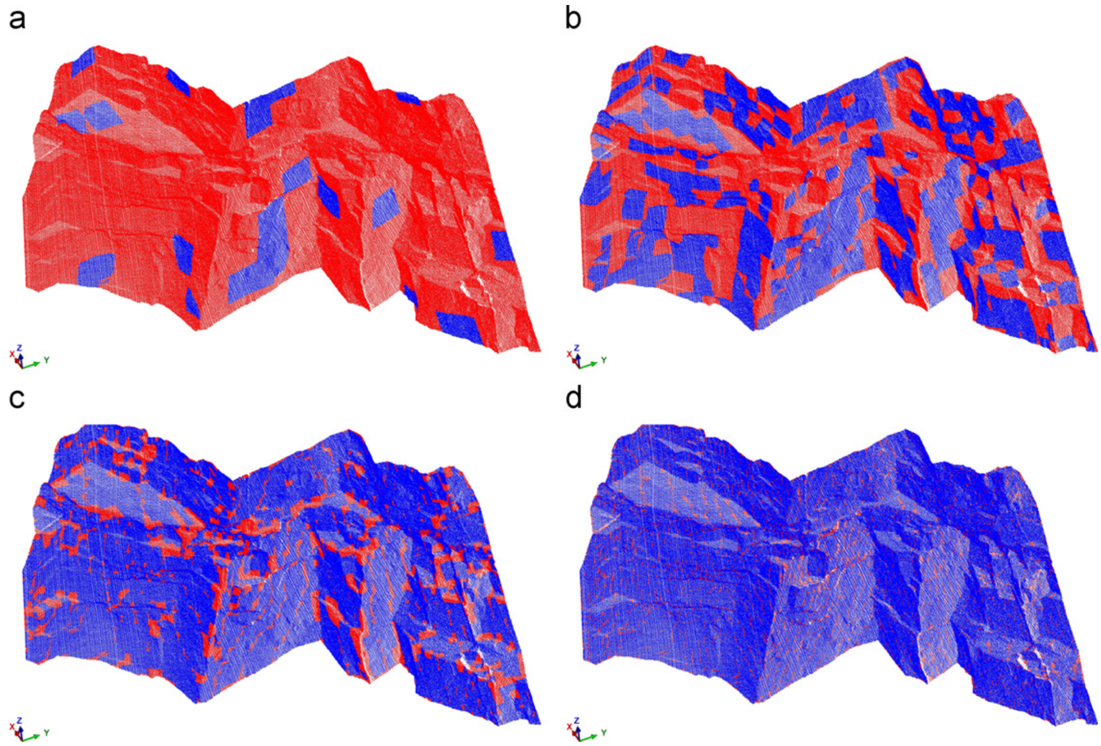

Fig. 3. Influence of the searching cube dimension on the total number of valid points (blue points) for a standard deviation threshold of 0.025 m. (a) 1 m selection cube; (b) 0.5 m selection cube; (c) 0.25 m selection cube and (d) 0.1 m selection cube. The areal extent of the point cloud is about 16 × 10 m. (For interpretation of the references to color in this figure legend, the reader is referred to the web version of this article.)

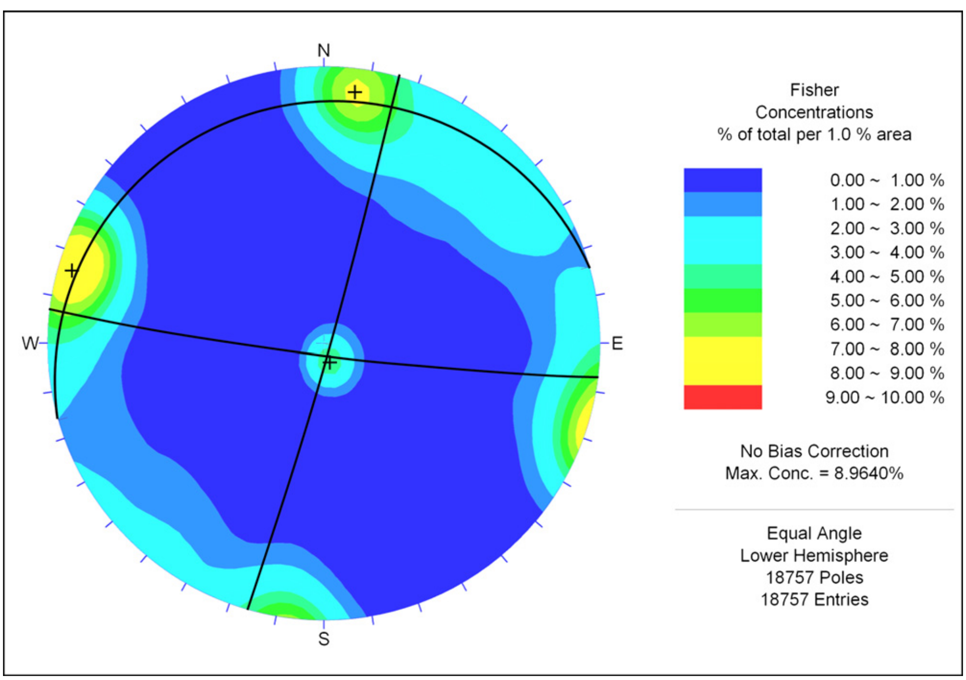

Fig. 4. Definition of the rock mass discontinuity sets on the stereographic projection. Contour lines have been obtained by plotting the orientation of valid clusters with a reference dimension of 0.1 m.

When all the points belonging to a discontinuity plane have been extracted, the dip and dip direction of the best fitting plane are computed, and the discontinuity bounding polygon is found (Fig. 7) by applying a convex hull algorithm [41].

Minimum and maximum discontinuity persistence can be, therefore, calculated for each set, based on the bounding polygon dimensions. This procedure fits well with the original definition of discontinuity persistence, which implies the areal extent of the surface [2]. It is important to emphasize that this method can produce an underestimation of the discontinuity persistence, as the exposed surface is often a sub-set of the entire fracture.

For each discontinuity a cylinder is drawn, with the axis perpendicular to the plane passing from the centroid and the base containing the surface points (Fig. 8).

By counting the number of discontinuities belonging to the same set intersected by the cylinder (hatched polygons, Fig. 8) and measuring the maximum distance between them (Fig. 8d) it is possible to assess the mean, minimum and maximum joint spacing, and the associated frequency of each set. If a set is defined to be infinitely persistent (i.e. bedding planes), its spacing is calculated by considering all the discontinuities belonging to that set, independently from their position.

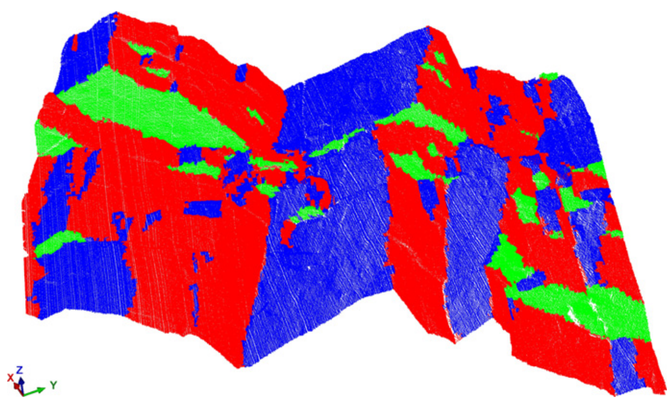

Fig. 5. Discontinuity set representation on the point cloud (Jn1: blue points; Jn2: red points; BG: green points). (For interpretation of the references to color in this figure legend, the reader is referred to the web version of this article.)

Block dimensions are evaluated by using the correlation proposed by Palmstrom [42,43]

$$V_b = \beta x J_v^{-3} \tag{4}$$

where J_v is the Volumetric Joint Count, defined by Palmstrom [44] and β is the block shape factor, which may be estimated by

$$\beta = 20 + 7\, a_3/a_1 \tag{5}$$

where a_1 and a_3 are the shortest and longest dimensions of the block, respectively.

Discontinuity roughness plays a very important role in the mechanical behavior of the rock mass, and the shear strength criteria for rock discontinuities include it among the basic parameters [45–47].

The most practical method for estimating the roughness of a discontinuity plane is by visual comparison of sampled roughness profiles with standard profiles published by Barton and Choubey [48].

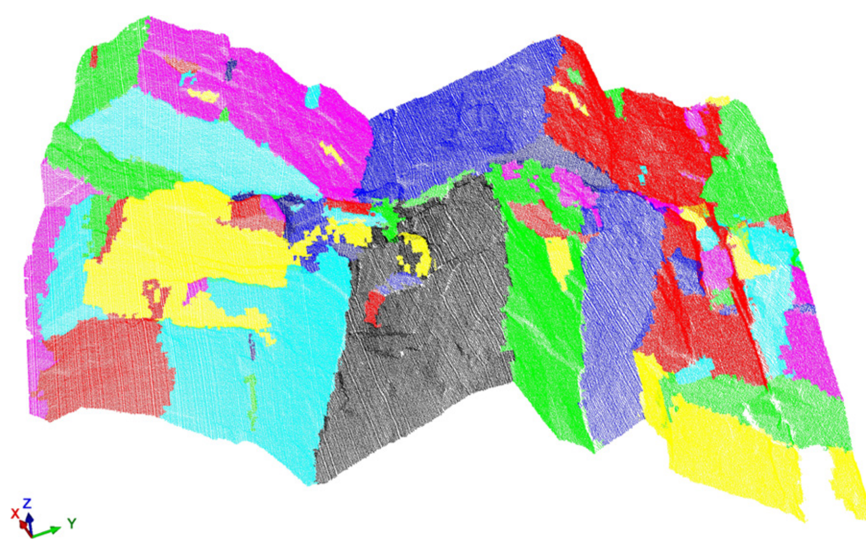

Fig. 6. Discontinuity plane detection from cluster merging.

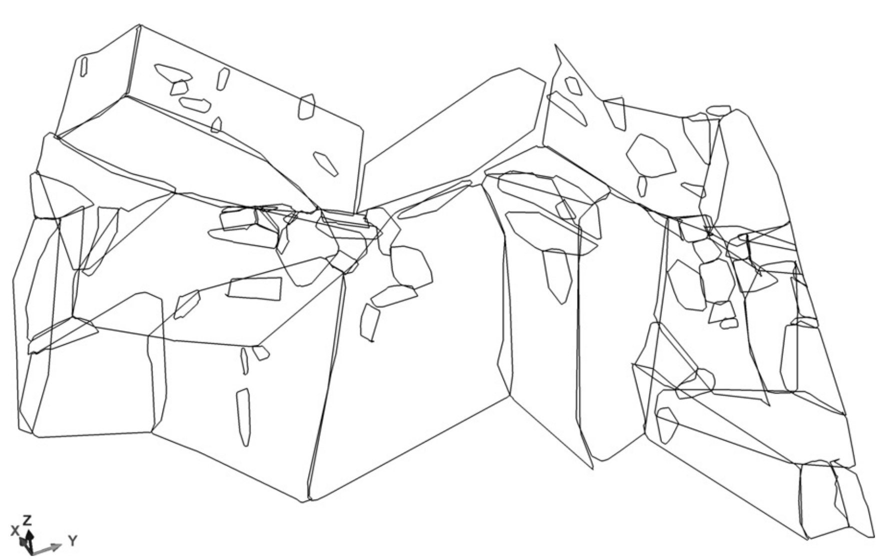

Fig. 7. Boundary polygons of identified discontinuities (Fig. 6).

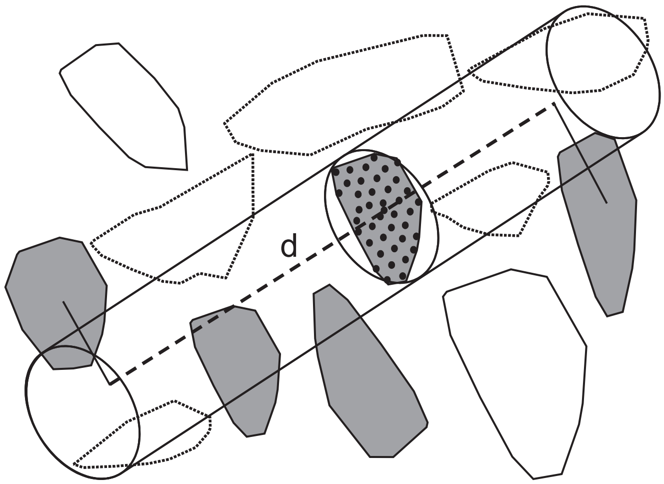

Fig. 8. Calculation of the true spacing and frequency of discontinuity sets. Continuous polygons: set 1; dashed polygons: set 2.

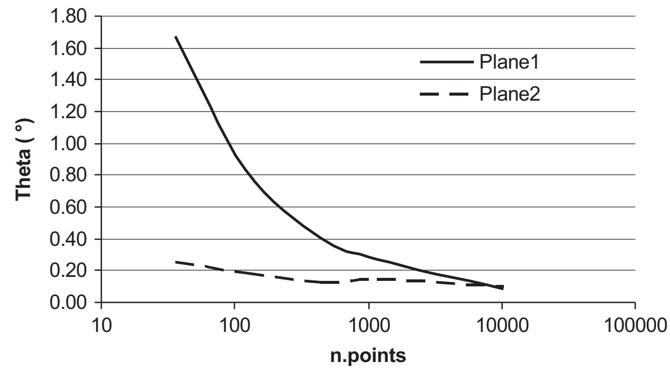

Fig. 9. Effect of instrument accuracy on the surface roughness estimation. Number of points within the selection vs. angular deviation between the original plane and the best fitting plane after the introduction of point range error.

Drawing roughness profiles of discontinuities directly from lidar data is a very difficult issue, due to limitations in instrument accuracy.

Moreover, it has been observed that discontinuity roughness is characterized by a very marked scale effect [49].

To overcome this problem a 3D approach can be pursued, as suggested by ISRM [2], by sampling the local surface orientation with a compass and disc clinometers with different diameters. This procedure requires however direct accessibility to the discontinuity plane and is quite time consuming, as a minimum number of 250 measures is suggested for the operation to be valid.

The proposed algorithm fits in well with these concepts and allows us to rapidly perform quantitative measures of the roughness of the main discontinuity surfaces at various scales.

A searching cube with different dimensions (0.1, 0.2, 0.4, 1, 2 m and maximum surface persistence) is moved along the selected discontinuity. If the number of points within the cube exceeds a prescribed threshold (to make sure the selection is centered on the surface), the best fitting plane dip and dip direction are obtained, and associated points are extracted from the surface. By plotting the orientation values on a stereoplot, the discontinuity roughness angles at various scales can be measured.

It is worth stressing that the reliability of this procedure depends mainly on the accuracy of the point cloud data; if it is too low, this could lead to an overestimation of surface roughness [50], especially for small scale analyses (0.1, 0.2 m), or low resolution point clouds.

To investigate the effect of instrument accuracy on the surface roughness estimation two virtual scans have been performed on hypothetical perfectly planar surfaces 0.1 m $\times$ 0.1 m wide. These have been located at a distance of 20 m from the observation point; the angle between the line of sight and the normal to the planes 1 and 2 were 0° and 75°, respectively. Each surface has been discretized in 36, 121, 441, 1156, 10,201 regularly spaced points and their position has been expressed in polar coordinates. Point range error has been added to the true values by considering a normal distribution with a standard deviation of 0.005 m, according to the experiments of Kersten et al. [51] for a Riegl LMS Z-420i instrument. Finally best fitting plane orientations have been calculated for all the corrected sets of points and the angles between each plane and the originals have been determined.

The results of this analysis (Fig. 9) show that the higher is the number of points within the selection, the lower is the angular deviation due to inaccurate measurements. This effect is attenuated if the angle between the line of sight and the normal to the plane is high (Plane 2; Fig. 9).

Fig. 10 reports the stereographic projection of the roughness characteristics for different reference dimensions, calculated for the black central discontinuity in Fig. 6. We can observe how the pole scattering decreases with increase in reference cube dimension (left). By drawing the contour lines of the poles for each reference dimension (right), we are able to quantitatively assess the surface roughness at different scales. For the smallest features (0.1, 0.2 m) the 95th percentile lines have been drawn to compensate the scattering due to the small number of points contained within the selections.

Regarding the remaining four ISRM parameters (aperture, seepage, wall strength and filling), their estimation requires direct access to the rock face and cannot be evaluated from conventional high resolution point clouds. Only centimetric joint apertures could be measured, based on the resolution and accuracy of original data; however, this capability has not been yet implemented within the presented algorithm.

By observing intensity colored point clouds obtained from laser scanning surveys, it could be also possible to qualitatively identify the seepage conditions of discontinuities, as wet areas are usually associated with lower reflectivity than dry ones. However, the reflectivity of a surface depends on many factors, such as the orientation related to the laser line of sight, the type of material and the distance from the scanner; thus, it is quite difficult to extract the wetness contribution, and to incorporate this capability within an automatic procedure.

One of the main difficulties arising when we process laser scanning data is the removal of noisy objects, such as vegetation, buildings, cables, piles, vehicles, pedestrians, etc.

If the shape of the object to be removed is regular, this operation can be easily performed by manually selecting the associated points and deleting them from the point cloud.

Vegetation is sometimes characterized by very irregular shapes; if bushes have to be removed on steep rock slopes, the manual procedure could take a very long time, and could bring to unsatisfactory results.

A specific option called *filterveg* has been implemented within the 3D version of the presented tool, for the removal of objects characterized by chaotic shapes. It consists of the iterative application of the first step of the 3D procedure described in this section with the aim of extracting clusters of points lying on regular surfaces, such as rock exposures.

With this option, after selecting specific cube dimensions and standard deviation thresholds and moving the searching cube along the point cloud, the segmentation is iterated by applying

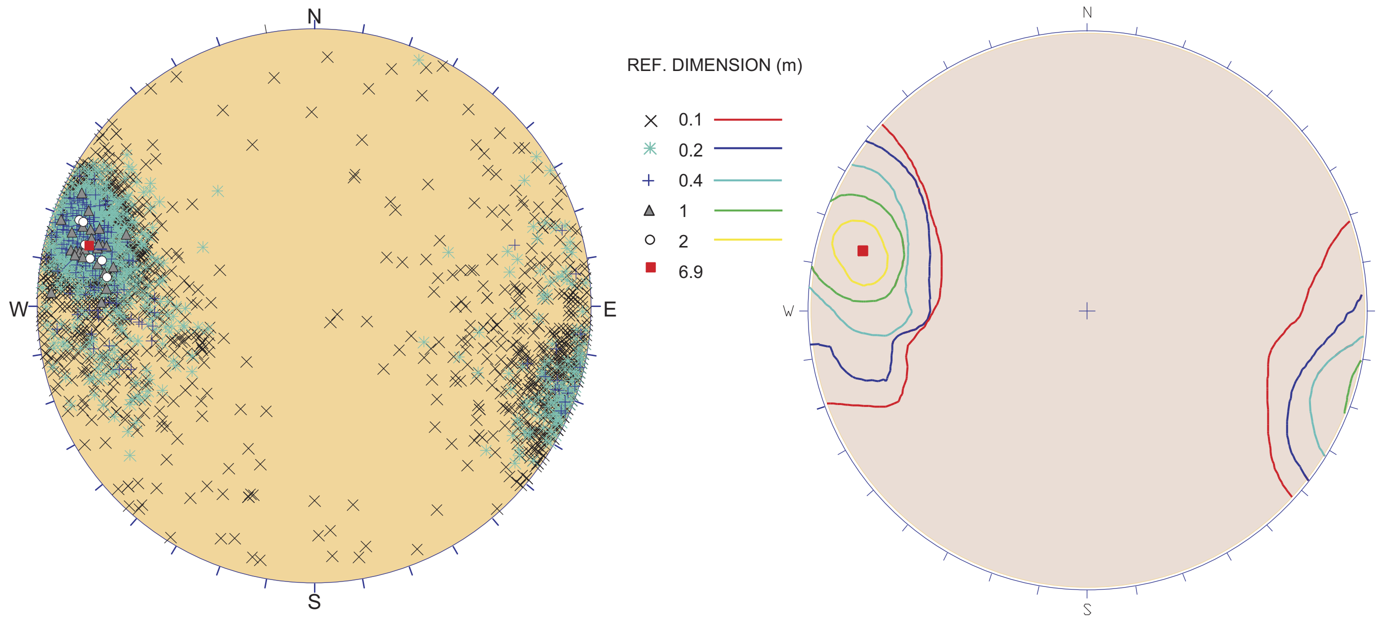

Fig. 10. Roughness characterization of the black discontinuity surface of Fig. 6: stereographic projection of poles (left) and contour lines of the poles for each reference dimension (right).

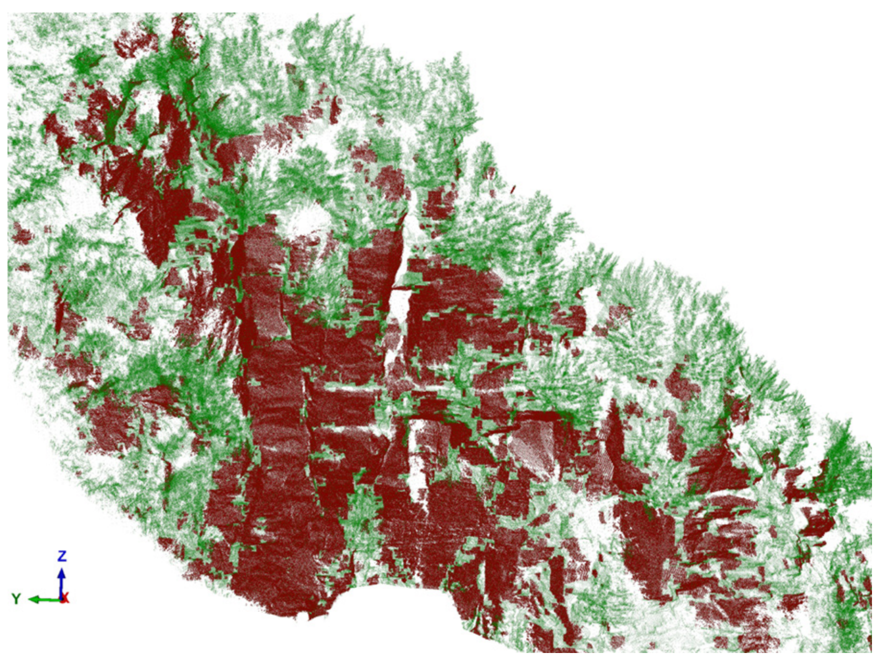

Fig. 11. DiAna application of the *filterveg* option for rock and vegetation segmentation.

different cube dimensions, with the result that even the smallest rock surfaces are extracted (Fig. 11).

3.2. DiAna2D

When a planar rock face has to be investigated, a 2D approach can be pursued by automatically extracting, or manually tracking, the discontinuity traces, and projecting them on the best fitting plane of the rock face [52,53].

With reference to the described 3D approach, we need to know in advance the orientations of the modal planes of each set, since we can not extract them from discontinuity traces. This information can be obtained either from a traditional geomechanical survey, or from the 3D analysis described in the previous section, performed on a rugged sector of the slope.

By measuring the length of the projected lines, discontinuity persistence can be evaluated for each trace [54]. It is important to remark that while measuring trace lengths will always produce a biased estimate of persistence in favor of the longest traces, the 3D approach is more objective, provided that a small enough reference cube dimension is selected.

Once the modal orientations of discontinuity sets are known, it is possible to associate each trace with the original set, by considering its trend and plunge (which are related to the pitch of the line on the reference plane). This approach is similar to the one adopted by Kemeny et al. [55].

The intersection lines between the fitting plane of the rock face and each discontinuity set plane are hence computed. If the angle between one of these intersections and the discontinuity traces is lower than a fixed threshold, the trace is assigned to the correspondent set.

In order to evaluate the joint frequency and spacing, virtual scanlines are drawn on the slope fitting plane, and apparent frequency and RQD [56] are calculated for each of them. It is possible to trace many scanlines, with different pitches on the rock face plane, in order to enhance the directional characteristic of these parameters.

Based on the scanline and discontinuity sets orientations, and on the coordinates of intersection points between discontinuity traces and the virtual scanlines, true spacing and associated frequency and mean persistence are then assessed for each set.

Finally, as described for the 3D version, block dimensions are evaluated using the correlation proposed by Palmstrom [42,43].

The 2D approach is suitable for analyzing rock masses with sharply distinct discontinuity sets and it could lead to misleading results when applied to rock masses with irregular block structure, or if important random discontinuities occur, in fact, the 2D association process of a trace to a discontinuity set is not unambiguous, since the same polyline can be attributed to more than one sets.

Although this is a weak point of the proposed approach, mainly considering photogrammetric methods, the 2D approach has been conceived as an integration to the 3D version.

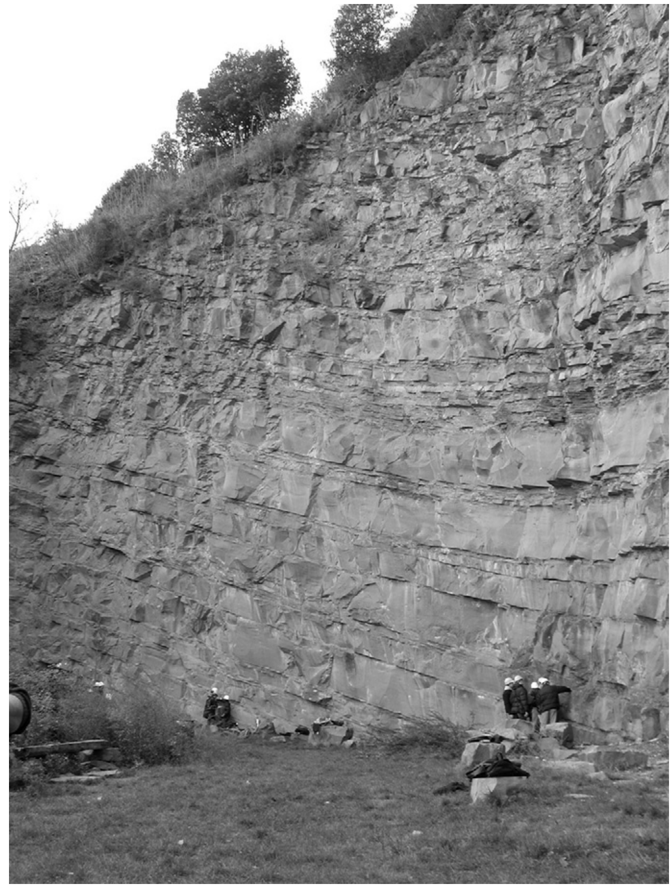

Fig. 12. The abandoned quarry of Maiano, near Florence.

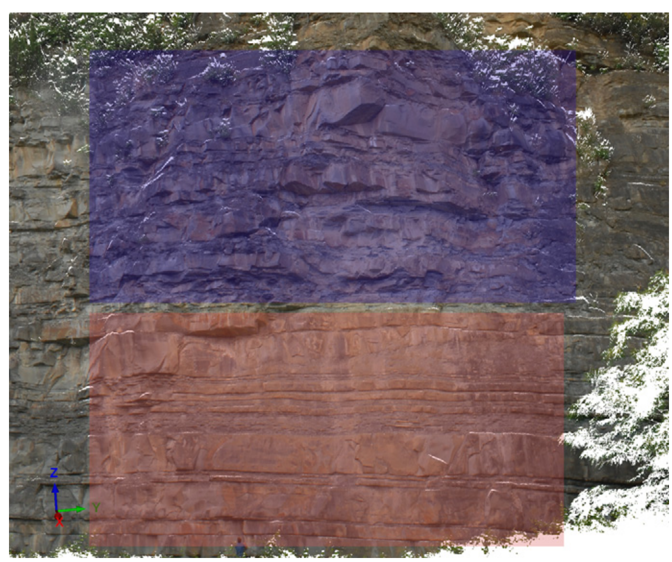

Fig. 13. True colored high resolution point cloud from laser scanning survey. The blue and red rectangles are the areas of application of the 3D and 2D approaches, respectively. The extent of the image is approximately 25 × 40 meters.

4. Field application

Both versions of the method have been applied for the geomechanical characterization of a man-made rock face near Florence (Fig. 12).

The abandoned quarry of Maiano is about 50 m high, and was one of the most important areas of extraction of a feldspathic greywacke, called Pietra Serena, belonging to the Monte Modino Sandstones [57]. This stone is one of the main materials employed in Florentine architecture from the 12th century, especially for decorative purposes [58].

The choice of this area is supported by the availability of traditional geomechanical survey data, by the presence of both planar and rugged surfaces in the lower and upper part of the eastern sector of the quarry, respectively (Fig. 13), and by the irregular block shapes within the rock mass, in order to apply the proposed methodology to a non-ideal real case, for enhancing its main advantages and disadvantages.

A detailed point cloud of the rock face has been obtained from a laser scanning survey. A long range 3D laser scanner (RIEGL LMSZ410-i) has been employed, based on the time of flight detection technique. This device is capable of determining the position of up to 12,000 points/s, with a maximum angular resolution of 0.008° and an accuracy of ±10 mm, from a maximum distance of 800 m. It is worth stressing that the accuracy specifications given for devices, which are built in small series (like laser scanners) may vary from instrument to instrument, and is often determined under controlled laboratory conditions [59].

In order to completely cover the rock face, two surveys from different scan positions have been performed. The resulting point clouds have been linked to a global reference system with the aid of reference points, the coordinates of which were defined by using a GPS device. A total of more than 3 million points and associated high resolution digital images have been taken. A true colored high resolution point cloud of the rock face is shown in Fig. 13.

A standard geomechanical survey has been performed, by applying the scanline method at the base of the rock wall. All the relevant parameters required to make a detailed description of the discontinuity system in the rock mass have been recorded on a specific form.

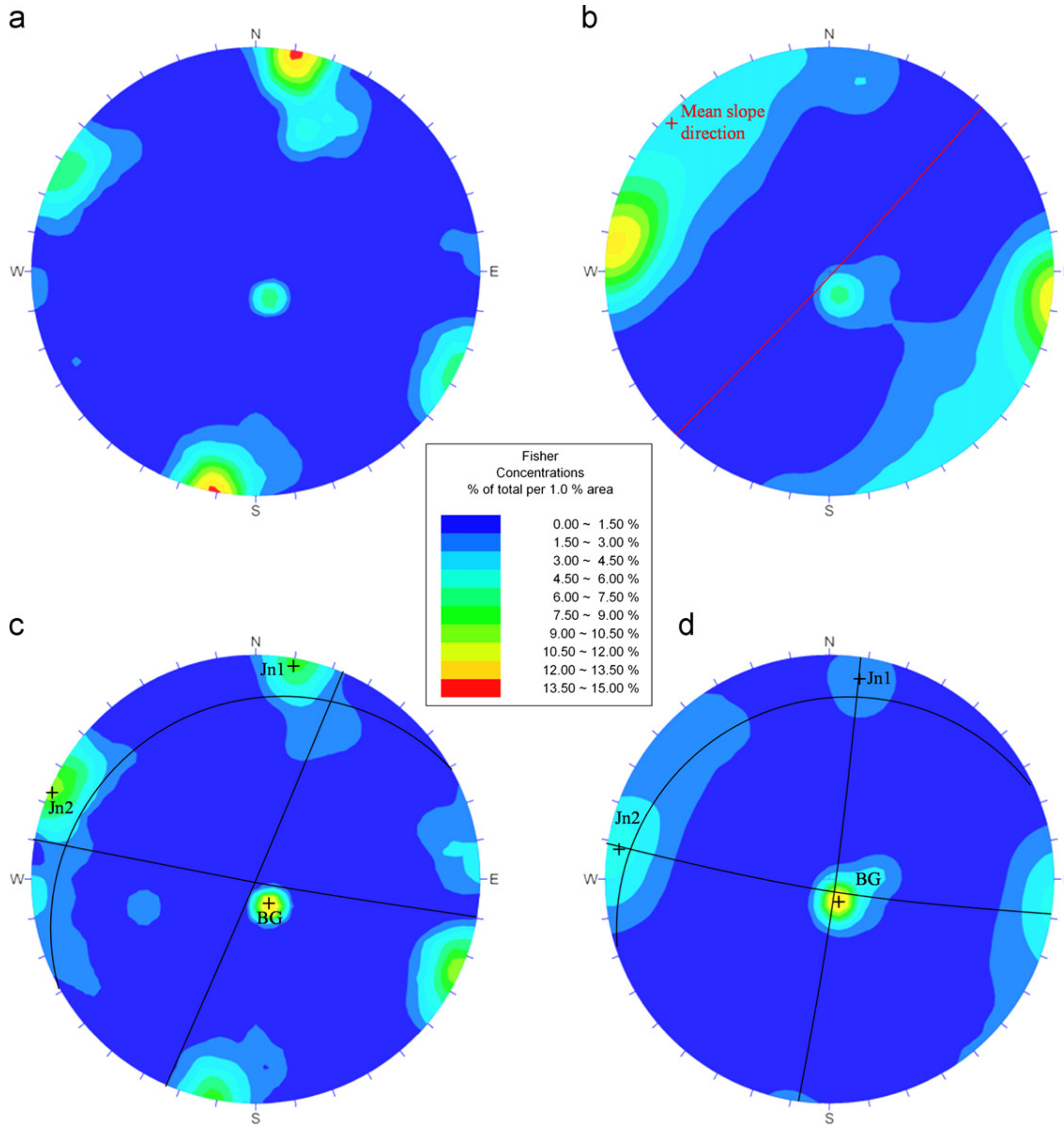

Fig. 14. (a) Stereoplot of discontinuities from traditional geomechanical survey; (b) semi-automatically extracted clusters from the high resolution point cloud; (c) field data, after Terzaghi correction; (d) numerical data, after inverse Terzaghi correction (see text).

Table 1
Comparison of the main geometrical parameters of discontinuities obtained from traditional field surveys, DiAna3D and DiAna2D analyses. X: true spacing; L: persistence; JRC: Joint Roughness Coefficient; V_b: Block volume.

	No. of sets	*Field survey* 3	*DiAna3D* 3	*DiAna2D* /
Jn1	dip/dip dir (°)	88/190	84/189	/
	X (m)	1.21	1.15	1.32
	L (m)	1.4	0.91	0.98
	JRC	10	Scale dep.	/
Jn2	dip/dip dir (°)	89/113	87/98	/
	X (m)	0.79	0.9	0.78
	L (m)	0.75	1.33	1.22
	JRC	11	Scale dep.	/
BG	dip/dip dir (°)	14/331	13/339	/
	X (m)	0.76	0.69	0.77
	L (m)	/	/	/
	JRC	10	Scale dep.	/
	V_b (m^3)	0.79	0.78	0.86

The orientation of all the sampled discontinuities is plotted on the stereographic projection in Fig. 14a using the Dips software [60]. The contour plot of Fig. 14c is the result of the Terzaghi correction [61] applied to field data; in the same plot discontinuity set poles and cyclographic traces have been drawn.

The resulting main geometrical properties of discontinuities are reported in Table 1.

The 3D approach has been tested on the blue area of Fig. 13. In order to extract as many features as possible from the point cloud, a small searching cube (side of 0.1 m) has been employed for the semi-automatic 3D analysis. The standard deviation threshold has been set to 0.01 m.

A total of 16,261 valid clusters have been obtained, and the contour lines of their orientations are projected on a stereoplot in Fig. 14b. While for traditional field surveys discontinuities sub-parallel to the scanline have lower probability to be sampled, the 3D analysis will favor those clusters perpendicular to the scan direction. For these reasons an inverse form of the Terzaghi correction, to compensate the bias introduced in favor of those features, which are perpendicular to the line of sight of the laser scanner, has been applied (Fig. 14d)

$$\omega = \frac{1}{|\cos\theta|} \quad (6)$$

where θ is the angle between the scan direction and the normal to the rock face.

By inspecting Fig. 14c and d, we can notice a good agreement between the set orientations measured in the field and the ones extracted semi-automatically. There is, in fact, a difference of about 15° in dip direction of set 2 (Jn2).

Fig. 14b shows a strong influence on the cluster concentration by the mean slope direction of the artificial slope. This contribution can be partially filtered by applying the Terzaghi correction (Fig. 14d).

After the extraction of the clusters (blue points in Fig. 15a), all valid points have been merged to obtain discontinuity sets (Fig. 15b) and discontinuity surfaces (Fig. 15c).

Fig. 15d represents the bounding polygons of the identified discontinuities.

It is worth stressing that, despite the small extension of discontinuities, their high roughness, and the irregular block shapes of the rock mass, the obtained results are very promising. They cannot be compared to an ideal case, where a regularly blocked rock mass occurs (Fig. 6). By observing Fig. 15b we can notice, for example, the accurate detection of the bedding plane set (red areas), which is characterized by very narrow (centimetric) and long (metric) discontinuity planes.

The geometrical properties of discontinuities retrieved with the 3D approach are reported in Table 1 and compared with those derived with standard scanline surveys performed in the field.

Joint roughness has been defined for the largest discontinuity surface of each set, according to the method described in the previous section.

The diagram of Fig. 16 (left) reports the roughness angle vs. the reference dimension, to enhance the scale effect. The stereoplot (Fig. 16, right) illustrates the pole scattering for the three surfaces, considering a 0.1 m reference cube.

Regarding the 2D analysis (Fig. 17), discontinuity traces (yellow lines) and virtual scanlines (blue lines) have been drawn on the best fitting plane of the quarry face in the lower sector of Fig. 13 (red area). The resulting geometrical properties of discontinuities are reported in Table 1.

It is worth stressing that the 2D approach does not allow to extract information on the number of sets and discontinuity orientation and roughness.

The estimation of the true spacing (X in Table 1) with both versions (2D and 3D) of the method is in good agreement with the results from the field survey.

Some differences however occur in connection with the persistence (L rows in Table 1); this could be explained by the practical difficulties in measuring the length of discontinuities in the field (since joint terminations are often difficult or impossible to reach); as a result discontinuity persistence is often roughly estimated rather than measured in the field.

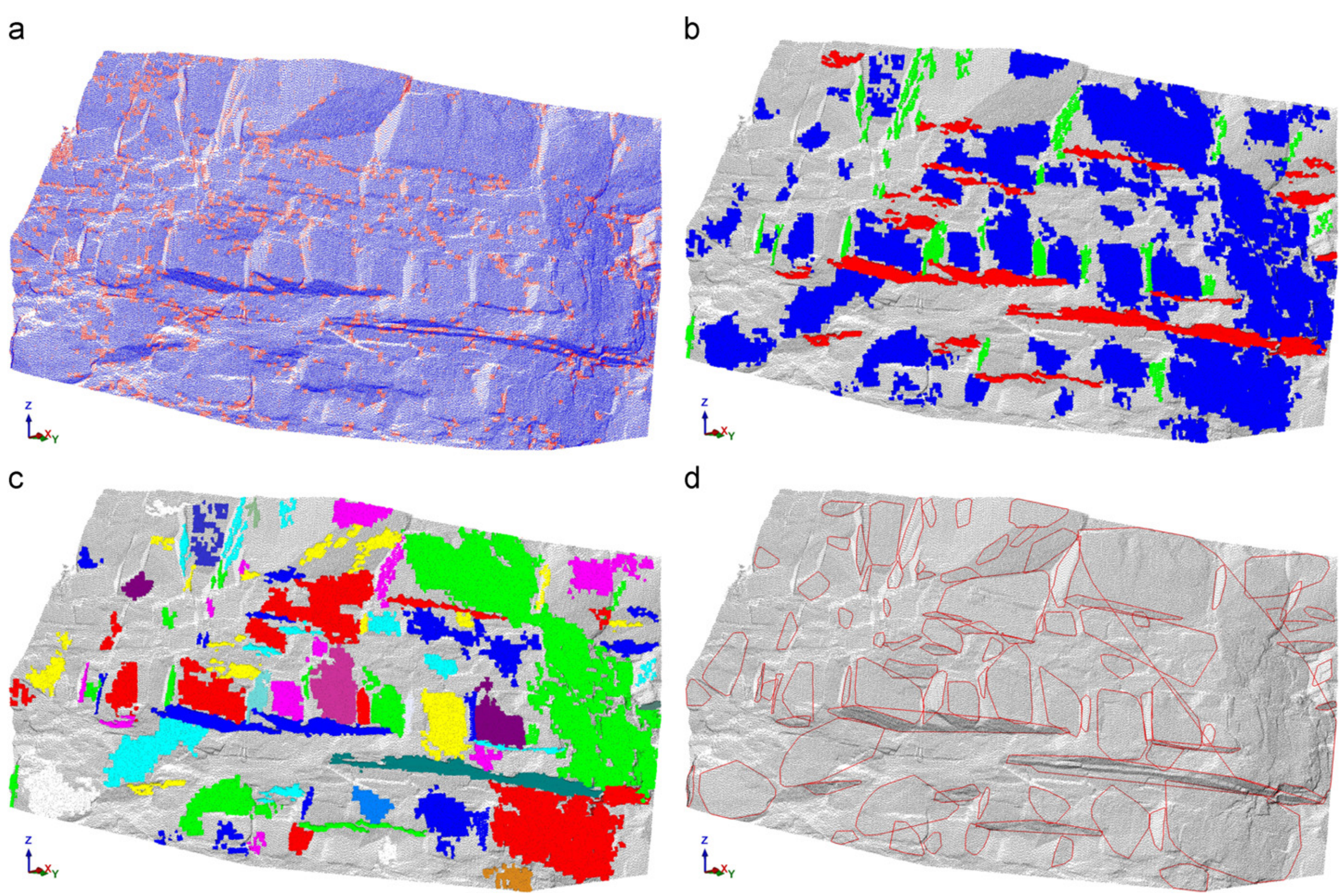

Fig. 15. DiAna 3D analysis results: (a) valid clusters (blue points) with 0.1 m reference dimension; (b) discontinuity set detection (green: Jn1; blue: Jn2; red: BG); (c) discontinuity plane detection; (d) representation of discontinuity boundary polygons.

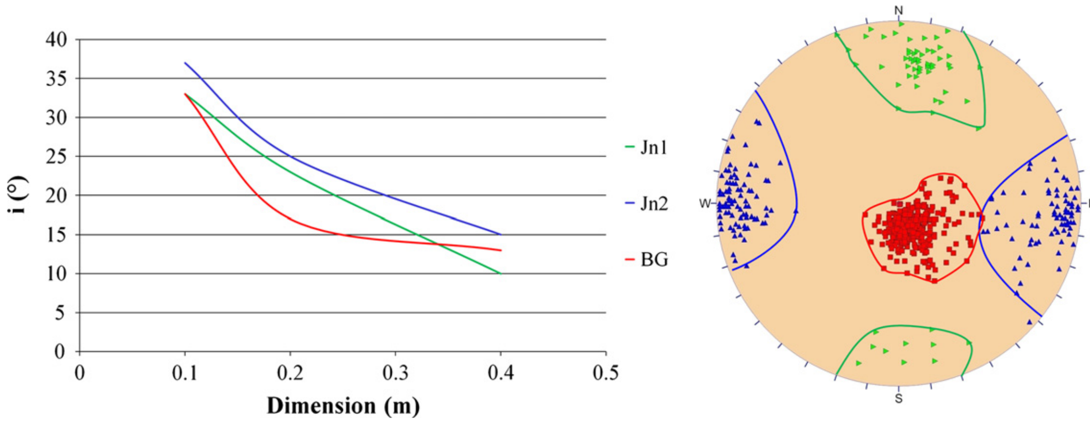

Fig. 16. Roughness estimation for the widest surface of each discontinuity set. Left: reference cube dimensions vs roughness angle diagram; right: Stereoplot of poles for a reference cube with 0.1 m dimension. Green: Jn1; blue: Jn2; red: BG.

Fig. 17. DiAna2D analysis. Discontinuity traces (yellow lines) and virtual scanlines (blue lines) on textured surface. (For interpretation of the references to color in this figure legend, the reader is referred to the web version of this article.)

5. Conclusions

With the aim of extracting 2D and 3D structural information from high resolution point clouds, a Matlab tool, called DiAna (Discontinuity Analysis) has been compiled.

The 3D approach is based on the definition of least squares fitting planes on clusters of points selected by moving in the space a searching cube with variable dimensions. If the associated standard deviation is below a defined threshold, the cluster is considered valid. By applying geometric criteria it is possible to join all the clusters lying on the same surface; in this way discontinuity planes can be reconstructed, and rock mass geometrical properties are calculated. One of the main outcomes of the described procedure is the definition of surface roughness at different scales. For low scales this operation is however limited by the accuracy of the point cloud.

The 2D approach is suitable for planar rock faces with no relief, and is based on the analysis of geometrical properties of discontinuity traces.

Six of the ten parameters suggested by ISRM [2] for the quantitative description of discontinuities (orientation, spacing, persistence, roughness, number of sets and block size) can be semi-automatically calculated with the proposed method. The remaining four parameters (aperture, seepage, wall strength and filling) cannot be assessed from conventional high resolution point clouds, as their estimation requires direct access to the rock face.

The presented method allows us to investigate larger portions of the rock mass related to field surveys, and all output parameters are quantitatively measured.

It is important to remark that a field analysis based on geologic experience is always required in order to validate the semi-automatically extracted data, especially if the rock mass is composed of different structural domains. In this case the semi-automatic procedure could give misleading results and is necessary to integrate the analysis with field data for a preliminary segmentation of the point cloud.

Finally, the proposed algorithm allows us to separate points belonging to a regular surface (such as rock face or ground) from irregular point geometries, typical of vegetation.

Both these versions have been applied to a real case, and the obtained properties have been compared with the results from a traditional geomechanical survey.

The results of this comparison are very promising, as all the computed parameters are in good agreement with the field ones.

References

[1] Priest SD. Discontinuity analysis for rock engineering. London: Chapman & Hall; 1993.

[2] ISRM. Suggested methods for the quantitative description of discontinuities in rock masses. International Journal of Rock Mechanics and Mining Sciences & Geomechanics Abstracts 1978;15:319–68.

[3] Chandler J. Effective application of automated digital photogrammetry for geomorphological research. Earth Surface Processes and Landforms 1999;24: 51–63.
[4] Lane SN, James TD, Crowell MD. Application of digital photogrammetry to complex topography for geomorphological research. Photogrammetric Record 2000;16:793–821.
[5] Kraus K, Pfeifer N. Determination of terrain models in wooded areas with airborne laser scanner data. ISPRS Journal of Photogrammetry and Remote Sensing 1998;53:193–203.
[6] Gigli G, Mugnai F, Leoni L, Casagli N. Analysis of deformations in historic urban areas using terrestrial laser scanning. Natural Hazards and Earth System Science 2009;9:1759–61.
[7] Ferretti A, Prati C, Rocca F. Multibaseline InSAR D.E.M. reconstruction: the wavelet approach. IEEE Transactions on Geoscience and Remote Sensing 1999;37:705–15.
[8] Oppikofer T., Jaboyedoff M., Blikra L.H., Derron M.H. Characterization and monitoring of the Åknes rockslide using terrestrial laser scanning. In: Proceedings of the 4th Canadian conference on geohazards: from causes to management. 2008. p. 211–18.
[9] Oppikofer T, Jaboyedoff M, Keusen HR. Collapse at the eastern Eiger flank in the Swiss Alps. Nature Geoscience 2008;1:531–5.
[10] Abellán A, Vilaplana JM, Martínez J. Application of a long-range terrestrial laser scanner to a detailed rockfall study at Vall de Núria (Eastern Pyrenees, Spain). Engineering Geology 2006;88:136–48.
[11] Lombardi L, Casagli N, Gigli G, Nocentini M. Verifica delle condizioni di sicurezza della S.P. Lodovica in seguito ai fenomeni di crollo nella cava di Sesto di Moriano (Lucca). Giornale di Geologia Applicata, AIGA 2006;3: 249–56. [In Italian].
[12] Jaboyedoff M, Couture R, Locat P. Structural analysis of Turtle Mountain (Alberta) using digital elevation model: toward a progressive failure. Geomorphology 2009;103:5–16.
[13] Fröhlich C, Mettenleiter M. Terrestrial laser scanning—new perspectives in 3D surveying. In: Thies M, Koch B, Spiecker H, Weinacker H, editors. Laser-scanners for forest and landscape assessment, 36. International Archives of Photogrammetry, Remote Sensing and Spatial Information Sciences; 2004. p. 8/W2.
[14] Vosselman G, Gorte BGH, Sithole G, Rabbani T. Recognizing structure in laser scanner point clouds. International Archives of Photogrammetry, Remote Sensing and Spatial Information Sciences 2004;46:33–8.
[15] Feng QH, Röshoff K. In-situ mapping and documentation of rock faces using a full-coverage 3-D laser scanning technique. International Journal of Rock Mechanics and Mining Sciences 2004;41:139–44.
[16] Roncella R, Forlani G, Remondino F. Photogrammetry for geological applications: automatic retrieval of discontinuity orientation in rock slopes. In: Videometrics IX, electronic imaging, IS&T/SPIE, Proceedings of the 17th annual symposium. 2005. p. 17–27.
[17] Slob S, Hack R, Van Knapen B, Turner K, Kemeny J. A method for automated discontinuity analysis of rock slopes with 3D laser scanning. Transportation Research Record 2005;1913:187–208.
[18] Turner AK, Kemeny J, Slob S, Hack R. Evaluation and management of unstable rock slopes by 3-D laser scanning. IAEG 2006;404:1–11.
[19] Voyat IH, Roncella R, Forlani G, Ferrero AM. Advanced techniques for geo structural surveys in modelling fractured rock masses: application to two Alpine sites. In: Tonon F, Kottenstette J, editors. Laser and photogrammetric methods for rock face characterization; 2006. p. 97–108.
[20] Jaboyedoff M, Metzger R, Oppikofer T, Couture R, Derron MH, Locat J, Turmel D. New insight techniques to analyze rock-slope relief using DEM and 3D-imaging cloud points: COLTOP-3D software. In: Rock mechanics: meeting society's challenges and demands. Proceedings of the 1st Canada–U.S. rock mechanics symposium, Vancouver, Canada, May 27–31, 2007,Eberhardt, E,Stead, D,Morrison, T, editors. London: Taylor & Francis. 2007. p. 61–8.
[21] Slob S, Hack R, Feng Q, Roshoff K, Turner AK. Fracture mapping using 3D laser scanning techniques. In: Proceedings of the 11th congress of the international society for rock mechanics: the second half century of rock mechanics, Lisbon, Portugal, vol. 1, 9–13 July, 2007. p. 299–302.
[22] Ferrero AM, Forlani G, Roncella R, Voyat HI. Advanced geostructural survey methods applied to rock mass characterization. Rock Mechanics and Rock Engineering 2009;42:631–65.
[23] Lato M, Diederichs MS, Hutchinson DJ, Harrap R. Optimization of LiDAR scanning and processing for automated structural evaluation of discontinuities in rockmasses. International Journal of Rock Mechanics & Mining Sciences 2009;46:194–9.
[24] Sturzenegger M, Stead D. Quantifying discontinuity orientation and persistence on high mountain rock slopes and large landslides using terrestrial remote sensing techniques. Natural Hazards and Earth System Science 2009;9: 267–87.
[25] Sturzenegger M, Stead D. Close-range terrestrial digital photogrammetry and terrestrial laser scanning for discontinuity characterization on rock cuts. Engineering Geology 2009;106:163–82.
[26] Maptek. Vulcan home page, 〈http://www.maptek.com/products/vulcan/index.html〉 (accessed August 2009).
[27] 3G Software and Measurement. Jointmetrix3D, home page, 〈http://www.3gsm.at/eng/jminfo_eng.asp〉 (accessed August 2009).
[28] Gemcom. Surpac, Geology and Mine Planning, home page, 〈http://www.gemcomsoftware.com/products/surpac/〉 (accessed August 2009).
[29] CSIRO. Sirovision, home page, 〈http://www.sirovision.com/〉 (accessed May 2010).
[30] Adam Technology. 3DM Analyst, Mining Analysis Software, home page, 〈http://www.adamtech.com.au/3dm/Analyst.html〉 (accessed August 2009).
[31] Split Engineering. Split-FX ver 2.0, home page, 〈http://www.spliteng.com/split-fx/〉 (accessed August 2009).
[32] Gexcel. 3DGeomec, home page, 〈http://www.gexcel.it/en/prodotti/3dgeomec〉 (accessed August 2009).
[33] Haneberg WC. 3-D rock mass characterization using terrestrial digital photogrammetry. AEG News 2006;49:12–5.
[34] Birch JS. Using 3DM analyst mine mapping suite for rock face characterization. In: Tonon F, Kottenstette J, editors. Laser and photogrammetric methods for rock face characterization; 2006. p. 13–32.
[35] Gaich A, Pötsch M, Schubert W. Basics, principles and applications of 3D imaging systems with conventional and high-resolution cameras. In: Tonon F, Kottenstette J, editors. Laser and photogrammetric methods for rock face characterization; 2006. p. 33–48.
[36] Haneberg WC. Using close range terrestrial digital photogrammetry for 3-D rock slope modeling and discontinuity mapping in the United States. Bulletin of Engineering Geology and the Environment 2008;67:457–69.
[37] Fischler MA, Bolles RC. Random sample consensus: a paradigm for model fitting with applications to image analysis and automated cartography. Comm of the ACM 1981;24:381–95.
[38] Sturzenegger M, Yan M, Stead D, Elmo D. Application and limitations of ground-based laser scanning in slope characterization. In: Eberhardt E, Stead D, Morrison T, editors. Proceedings of the 1st Canadian US rock mechanics symposium. London: Taylor & Francis; 2007. p. 29–36.
[39] MathWorks. MATLAB, the language of technical computing. Version 7.5 Release 2007a. [CD-ROM]. Mathworks Inc.
[40] Golub GH, Reinsch C. Singular value decomposition and least squares solutions. Numerische Mathematik 1970;14:403–20.
[41] Preparata FP, Hong SJ. Convex hulls of finite sets of points in two and three dimensions. Communications of the Association for Computing Machinery 1977;20:87–93.
[42] Palmstrom A. RMi—a rock mass characterization system for rock engineering purposes. PhD thesis 1995, University of Oslo, Department of Geology, 400 pp.
[43] Palmstrom A. Measurement of correlations between block size and rock quality designation (RQD). Tunnelling and Underground Space Technology 2005;20:362–77.
[44] Palmstrom, A. The volumetric joint count—a useful and simple measure of the degree of jointing. In: Proceedings of the 4th international congress IAEG, New Delhi. vol. 5. 1982. p. 221–8.
[45] Patton FD. Multiple modes of shear failure in rock. In: Proceedings of the 1st congress of the international society of rock mechanics, Lisbon. vol. 1. 1966. p. 509–13.
[46] Barton NR. Review of a new shear strength criterion for rock joints. Engineering Geology 1973;7:287–332.
[47] Barton NR. The shear strength of rock and rock joints. International Journal of Rock Mechanics and Mining Sciences & Geomechanics Abstracts 1976;13:1–24.
[48] Barton NR, Choubey V. The shear strength of rock joints in theory and practice. Rock Mechanics 1977;10:1–54.
[49] Barton NR, Bandis S. Effects of block size on the shear behavior of jointed rock. Keynote lecture. In: Proceedings of the 23rd U.S. symposium on rock mechanics. 1982. p. 739–60.
[50] Rahman Z, Slob S, Hack R. Deriving roughness characteristics of rock mass discontinuities from terrestrial laser scan data. Proceedings of the 10th IAEG Congress, "Engineering geology for tomorrow's cities". Nottingham, United Kingdom: Geological Society of London; 6-10 September 2006 paper 437, 12 pp.
[51] Kersten T, Mechelke K, Lindstaedt M, Sternbernberg H. Geometric accuracy investigations of latest terrestrial laser scanning systems. In: Proceedings of FIG Working Week, Stockholm, Sweden. 2008. On CD-ROM.
[52] Reid TR, Harrison JP. A semi-automated methodology for discontinuity trace detection in digital images of rock mass exposures. International Journal of Rock Mechanics and Mining Sciences 2000;37:1073–89.
[53] Lemy F, Hadjigeorgiou J. Discontinuity trace map construction using photographs of rock exposures. International Journal of Rock Mechanics and Mining Sciences 2003;40:903–17.
[54] Priest SD, Hudson JA. Estimation of discontinuity spacing and trace length using scanline surveys. International Journal of Rock Mechanics and Mining Sciences & Geomechanics Abstracts 1981;18:183–97.
[55] Kemeny J, Turner K, Norton B. In: Tonon F, Kottenstette J, editors. LIDAR for rock mass characterization: hardware, software, accuracy and best-practices In: Laser and photogrammetric methods for rock face characterization; 2006. p. 49–61.
[56] Deere DU. Technical description of rock cores for engineering purposes. Felsmechanik und Ingenieurgeologie 1963;1:16–22.
[57] Abbate E, Bruni P. Modino-Cervarola. Torbiditi oligo-mioceniche ed evoluzione del margine nord appenninico. Memorie della Società Geologica Italiana 1987;39:19–33. [In Italian].
[58] Bastogi M, Geologia Fratini F. litologia, cave e deterioramento delle pietre fiorentine. Memorie descrittive della Carte Geologica d'Italia 2004;66: 27–42. [In Italian].
[59] Bohler W, Bordas VM, Marbs A. Investigating laser scanner accuracy. International Archives of Photogrammetry and Remote Sensing 2003;34:696–701.
[60] Rocscience. Dips, graphical and statistical analysis of orientation data, Ver. 5.0, User's manual; 2003.
[61] Terzaghi RD. Source of error in joint surveys. Geotechnique 1965;15:287–304.